Chapter 5

Experimental Results and Discussion

5.1 Introduction

The aim of the thesis is to fabricate a subwavelength metal grating with high light separation efficiency for the visible spectra (0.4 um ~ 0.8 um) and the entire near infrared spectra (0.8 um ~ 2.5 um). To accommodate to available facilities, the feasibility of proposed processes will be demonstrated by the molds with the period around 200 nm. First, the master mold process (using the interferometric lithography and the e-beam lithography individually), the remolding process (PDMS mold conversion) and the imprint process (UV-nanoimprint lithography) will be demonstrated in turn. For the master mold process, two samples with different specifications will be presented. Sample I fabricated by interferometric lithography is the grating with a period of 200 nm, and sample II fabricated by e-beam lithography is the grating with period of 600 nm. Thereafter, the measured performance of wire grid polarizer (the function of light separation) will be reported.

5.2 Results of Master Mold

Two master molds, sample I and sample II, were fabricated by interferometric lithography and e-beam lithography, respectively. The process and examination of both molds are discribed as follows.

5.2.1 Interferometric Lithography --- Sample I

Interferometric lithography was utilized to fabricate the nanostructure. The thickness of photoresist and the exposure dose were two key factors of this process. EPK-731 was used to be the photoresist. From the specification of EPK-731, if the thickness of photoresist was 348 nm, the exposure dose was 24 mJ/cm^2.

Argon Laser of wavelength 244 nm was utilized as the source of exposure. From Eq. 3.2.4, varying the incident angle could vary the grating period. Take the grating we made as example. If the grating period is about 351 nm, the angle of incidence in interferometric lithography should be about 20.34°. If the grating period is decreased to 200 nm, the angle of incidence in interferometric lithography is about 37.6°.

The photoresist grating is fabricated after post exposure baking and developing. For sample I, the interference period is about 200 nm. The area of interference is about 1 cm^2 limited by the size of the optics used. The AFM result of the grating is shown in Fig. 5.1. The period and the depth of the grating are 226 nm and 40 nm, respectively.

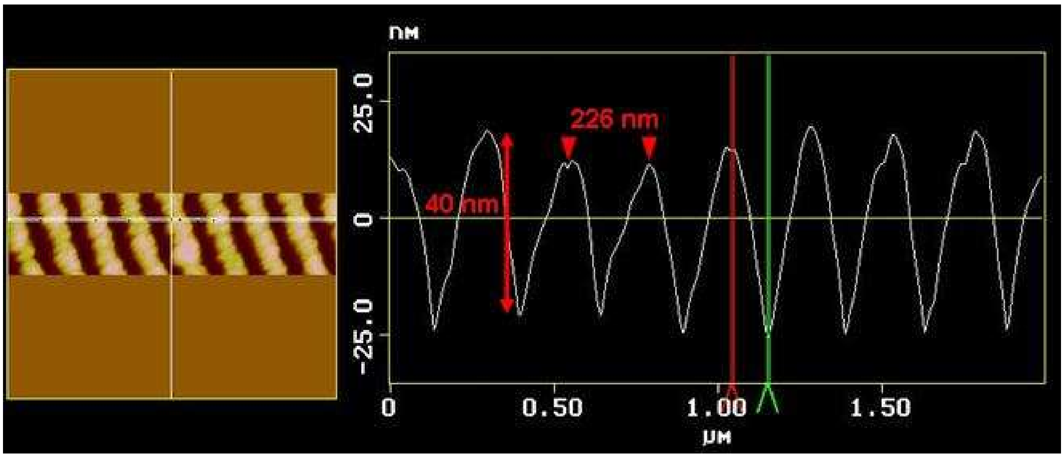

Fig. 5.1 AFM images of the photoresist grating with 200 nm period

5.2.2 E-beam Lithography --- Sample II

For sample II, e-beam lithography was utilzed to fabricate the master mold with 600 nm period. However, the area of grating was much smaller than that of sample I. The AFM result of the grating is shown in Fig. 5.2. The period and the depth of the grating were 609 nm and 40 nm, respectively. The SEM result of the grating is shown in Fig. 5.3. The picture shows the top view of the fabricated sub-wavelength grating. The period and aperture size are found to be 591 nm and 234 nm respectively.

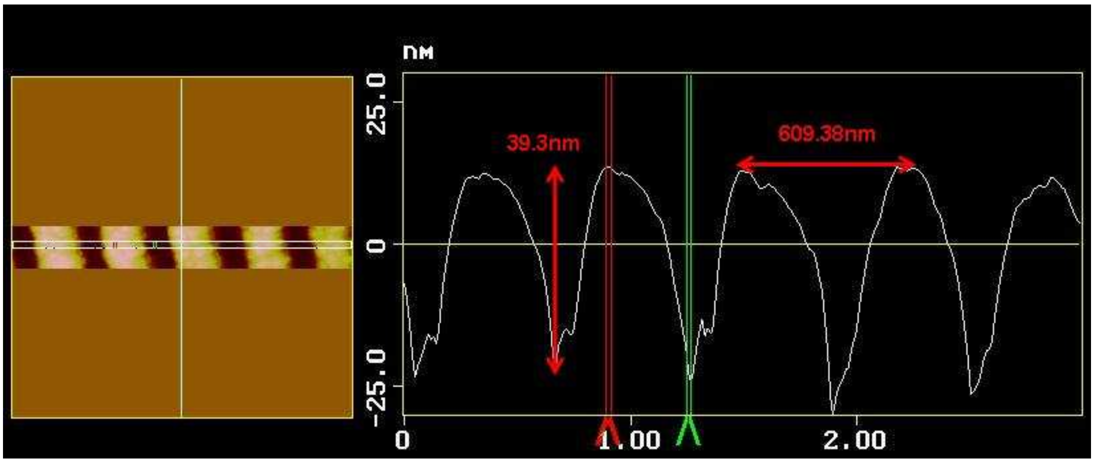

Fig. 5.2 AFM images of the photoresist grating with 600 nm period

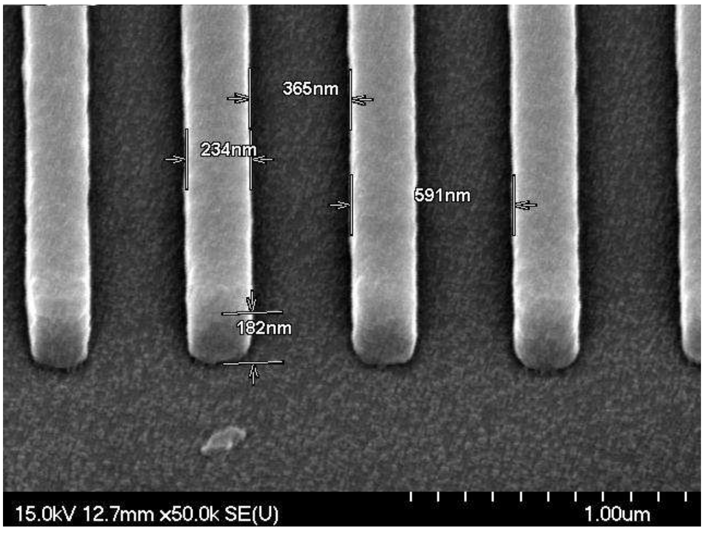

Fig. 5.3 SEM image of the top view of the photoresist grating with 600 nm period

5.3 Results of Replicated PDMS Mold

Both master molds fabricated by interferometry and e-beam lithography need to be converted as PDMS molds because transparent molds are necessary for the next step of UV-nanoimprint lithography. In our experiment, PDMS showed the high adhesion ability with the photoresist, leading to the failure of PDMS-releasing. Therefore, a mold release layer was necessary. Owing to the low surface energy, Cr or SiO_2 was sputtered onto the photoresist grating (~ 5 nm thick) as the mold release layer to facilitate the PDMS-release process.

In the PDMS conversion process, the other key issue lies in the step of creation of vacuum. Here, the grating with 700 nm period and 40 nm depth is utilized to demonstrate the necessity of creation of vacuum. The results are shown in Tab. 5.1, where the comparsion of the PDMS conversion processes with vacuum. The first row shows the original master mold. The period is 700 nm and the depth is 40 nm. The second row is the result of the converted PDMS without vacuum. It shows that the period has been expanded and the duplicated structure has distortion. Because the structure of the master mold is very subtle, it is difficult for the colloid to permeate the structure. Besides, the bubbles in the gap would cause the defect of the structure. Therefore, we take advantage of vacuum to improve the quality of the PDMS mold. The third row shows the result after PDMS conversion with vacuum. We can find that the duplicated structure is better than the previous case and the period is closer to the original one. Comparing the PDMS molds converted with and without vacuum treatment, we find that the conversion processes with vacuum can produce better structure of PDMS molds.

Tab. 5.1 Comparsion of PDMS conversion with vacuum

(1) Original master mold	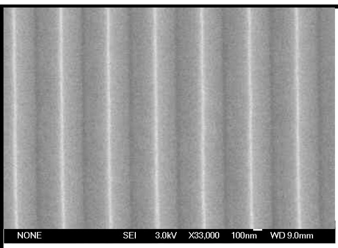	• Period:~700nm • Depth:~40nm
(2) PDMS result without vacuum	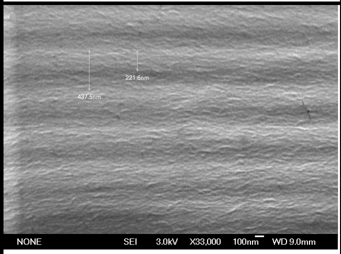	• Period expansion • Duplicated structure is distortion
(3) PDMS result With vacuum	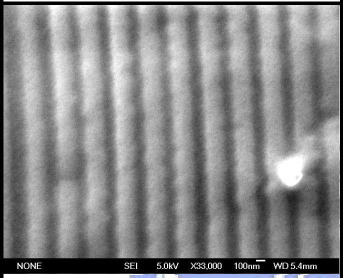	• Duplicated structure is better than prior case • Period is more close to original mold

For sample I, the PDMS replica mold with the grating period of 200 nm is fabricated, as shown in Fig. 5.4. The area of PDMS mold is also about 1 cm^2 as the photoresist grating. The period and the depth of the mold are 223 nm and 32 nm, respectively.

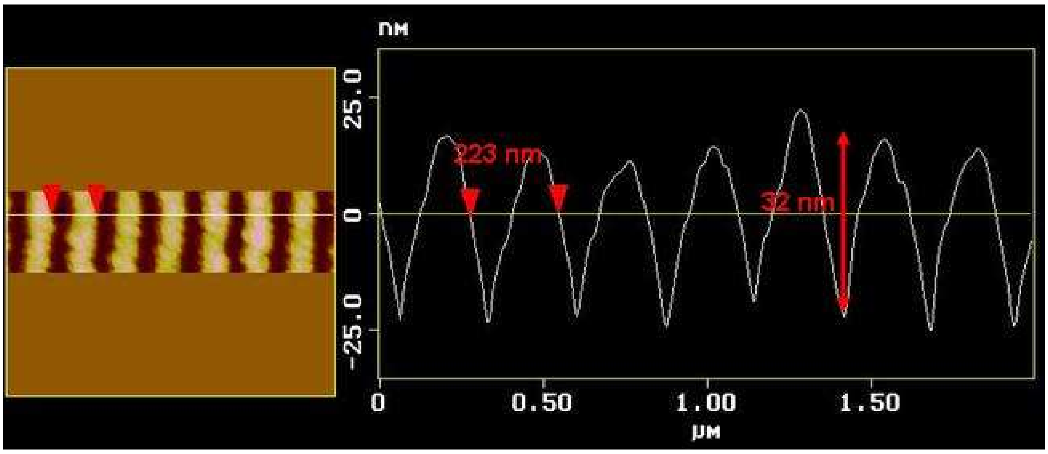

Fig. 5.4 AFM images of the PDMS mold with 200 nm period

For sample II, the PDMS replica mold of the grating with 600 nm is then fabricated, as shown in Fig. 5.5. The area of PDMS mold is also about 0.01 cm^2 which is limited by the size of e-beam lithography. The period and the depth of the mold are 598 nm and 56 nm, respectively.

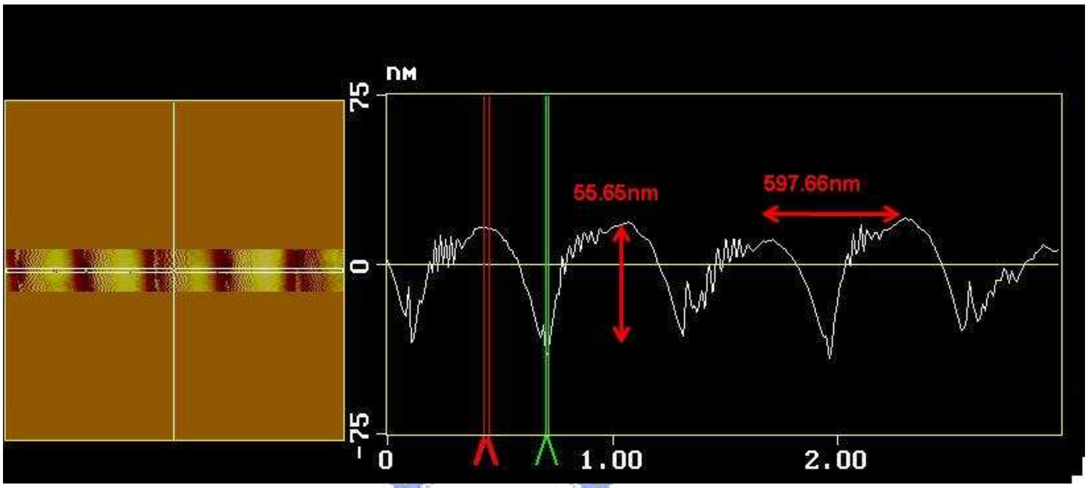

Fig. 5.5 AFM images of the PDMS mold with 600 nm period

5.4 Results of UV-nanoimprint Lithography

After the remolding process, the replicated PDMS mold is then utilized for the UV-nanoimprint lithography to transfer the nano-structure to the designate material, which is a photoresist: mr-L 6000.5. The details of fabrication have been described in section 3.5.4. By using the process shown in Fig. 3.8, the photoresist with nano-grating patterns can be fabricated after the mold releasing procedure. For the case of sample I, the photoresist grating with 200 nm period is fabricated by UV-nanoimprint, as shown in Fig. 5.6(a). The period and the depth of the grating are measured as 0.2 μm and 40 nm, respectively. Besides, the thickness of residual resist is about 200 nm. On the other hand, for sample II, the photoresist grating with 600 nm period was fabricated by UV-nanoimprint, as shown in Fig. 5.6(b). The period and the depth of the grating were 571 nm and 144 nm, respectively. The thickness of residual resist is about 312 nm.

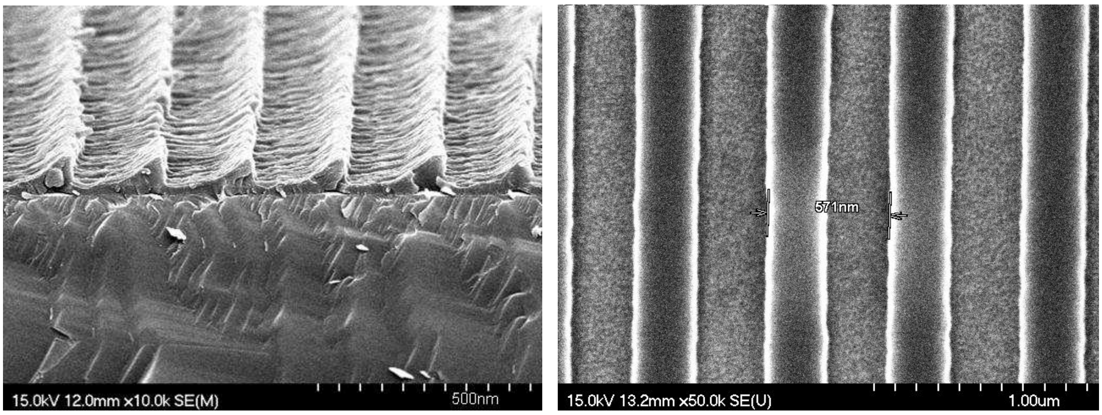

(a) (b)

Fig. 5.6 SEM results of the photoresist grating after the UV-nanoimprint (a) Sample I (b) Sample II

During the imprint process, some issues occur. For instance, when nitrogen is applied to pressurize the PDMS during the imprint process, the pattern closed to the edge distorts seriously. Fig. 5.7 illustrates the operation of imprint process. Because there is a gap between the PET film and the imprint surface, when the gas pressure increases, the side force will also press the sidewall. Therefore, the edge of the PDMS was distorted seriously during imprint, leading to ununiform imprinted results, as shown in Fig. 5.8.

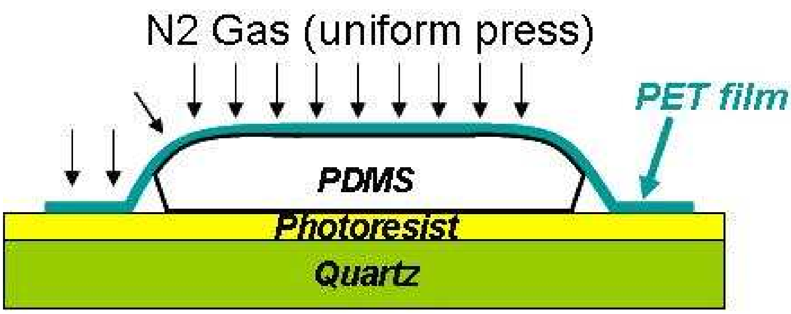

Fig. 5.7 Operation of imprint process

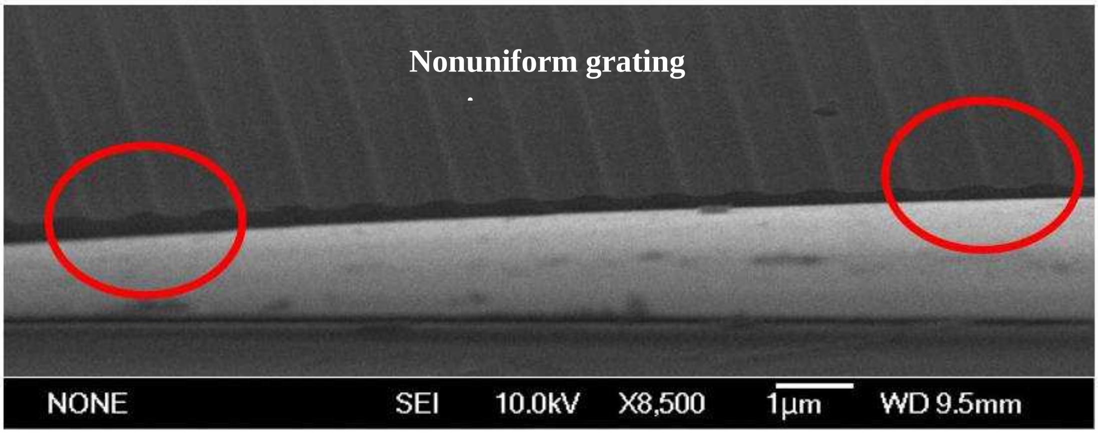

Fig. 5.8 Imprint result

In order to prevent the distortion of the PDMS mold, an Al holder is utilized. The holder is hollow and the inner area of the holder is almost the same as that of the PDMS mold. During the imprint, the PDMS mold clutched via the holder will be put on the resist. The side view of the imprint specimen with the PDMS mold and the holder is illustrated in Fig.5.9. The function of the holder is to transfer the side force to the holder, preventing side force on PDMS. Therefore, the distortion at the boundary shall be improved.

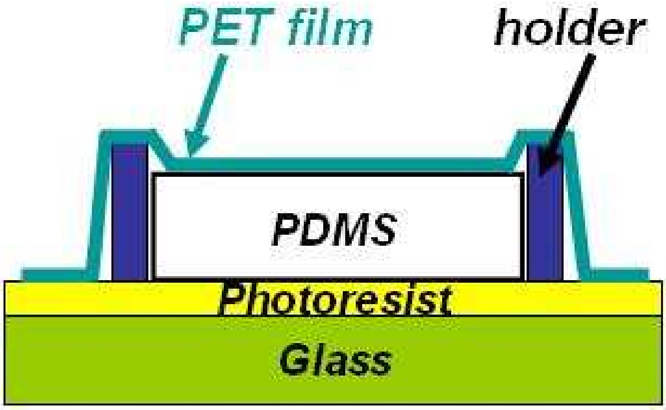

Fig. 5.9 Imprint process using the proposed holder

The uniformity of imprinted results is then analyzed. The uniformity is defined as the minimum depth over the average depth, and the experimental result is about 88%, as shown in Fig. 5.10. It shows that although a holder has been applied, the improvement of uniformity remains unsatisfying.

To further improve the uniformity, we looked for other factors which affect uniformity. From our investigations, the thickness of PDMS and the way of pressurization influence the imprint. Therefore, we control the thickness of PDMS to be lightly thinner than that of the holder; meanwhile, we apply the gas to imprint slowly and smoothly. The improved result of imprint is shown in Fig. 5.11. It is obviously that the imprinted results become more uniform (as the measured heights of the middle and edge parts), and the uniformity is imrpoved to be 98%.

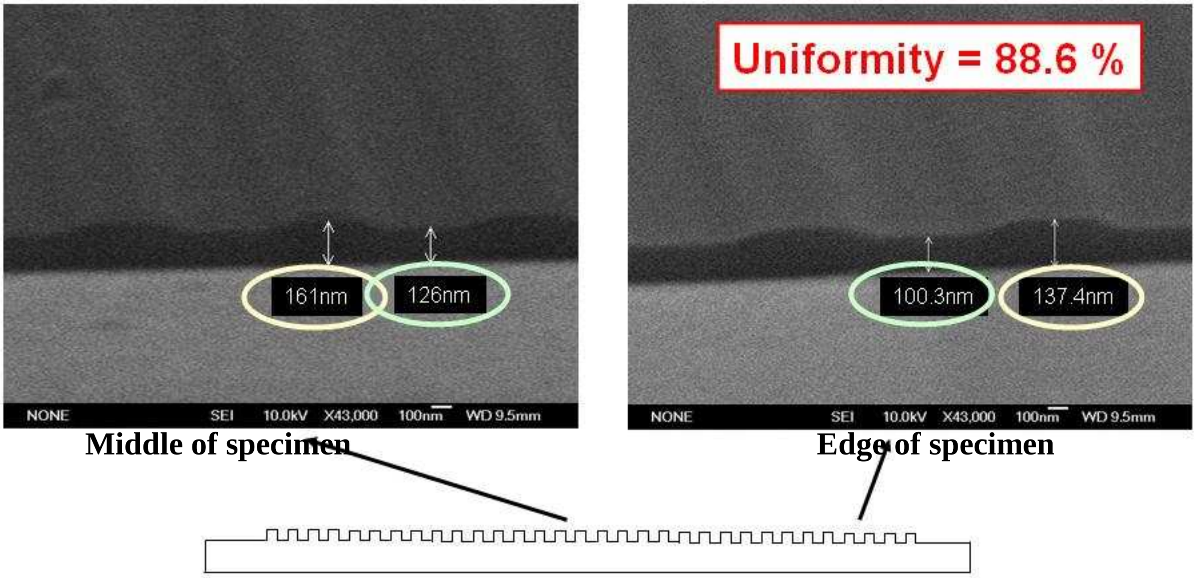

Fig. 5.10 Uniformity of imprint by using a holder

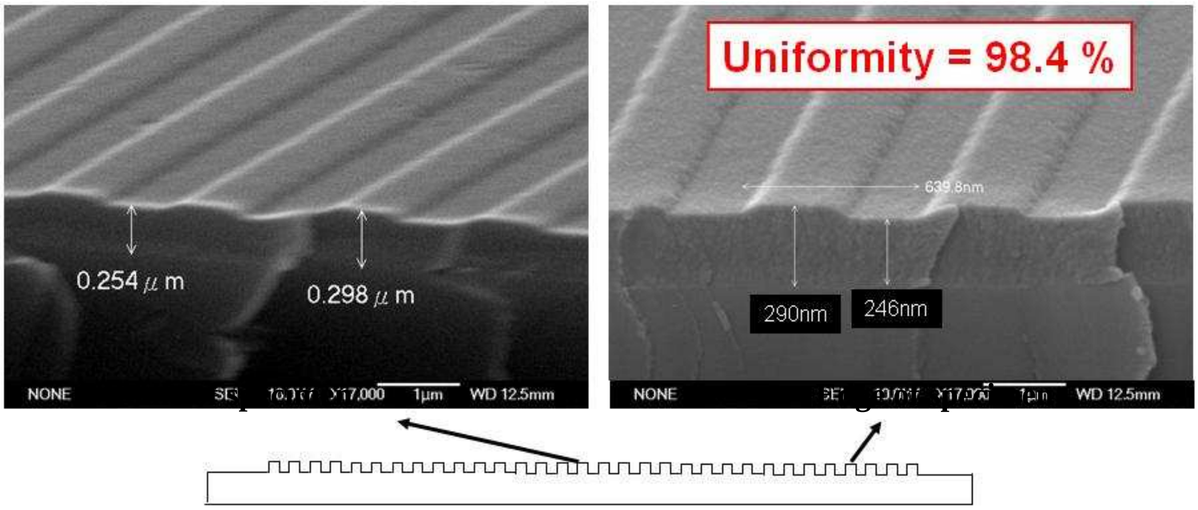

Fig. 5.11 Uniformity of imprint improved by controlling the PDMS's thickness and the pressurized process

5.5 Results of Oblique E-beam Evaporation

Oblique e-beam evaporation is proposed to fabricate the wire grid polarizer. A metal fixture is used to make the sample tilt with an angle θ during evaporation. Assume the grating length is infinity and the grating period is P, as shown in Fig. 5.12. For the ideal case, the fill factor $\boldsymbol{F = A/P = (P-H*\cot\theta)/P}$, where A is the width which Al has covered per period and H is the grating depth. Since the fill factor **F** is the function of the tilt angle, the evaporation result will vary as the tilt angle changes. Ideally, the proposed evaporated result as shown in Fig. 5.13 shall occur with the tile angle θ is 83.48° for the case of the period and the depth as 700 nm and 40 nm, respectively. Theoretically, θ can be derived from the relationship between the desired depth and the grating period.

$$\tan\theta = \frac{p/2}{depth} = \frac{350nm}{40nm} = 8.75 \qquad 5.5.1$$

$$\theta = \tan^{-1}(8.75) = 83.48° \qquad 5.5.2$$

And the smaller tilt angle θ is, the wider area of Al covered is.

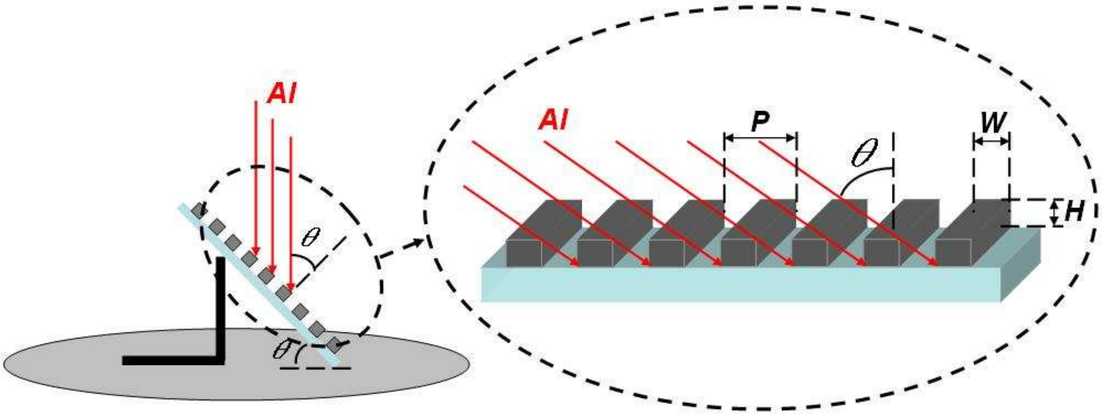

Fig. 5.12 Parameters of oblique evaporation

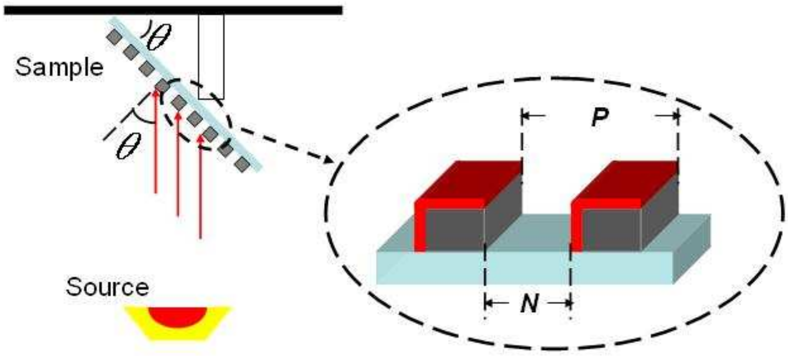

Fig. 5.13 The proposed evaporated result

In experiment, the period and the depth of photoresist grating are designed as 700 nm and 300 nm, respectively. Assume that the evaporation thickness of Al is 50 nm and the tilt angle is changed from 50° to 85°. The evaporation results with different title angles are shown in Tab.5.2. According to the results, the Al-covered area is enlarged as the tile angle decreases. The whole surface is covered with Al when the tilt angle is less than 50°. On the other hand, the depth after evaporation is also a function of tilt angle. The measured results demonstrated that the depth decreases as the tilt angle decreases, in agreed with the design.

Tab. 5.2 Evaporation results with different title angle θ

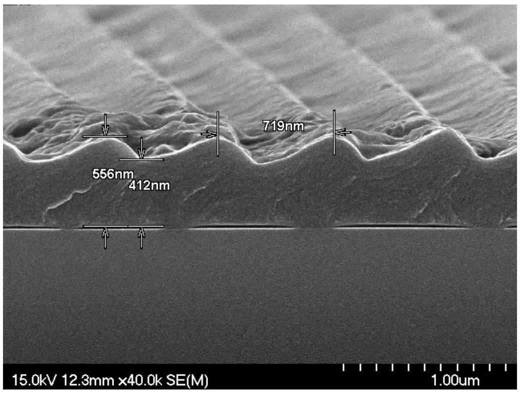 Original	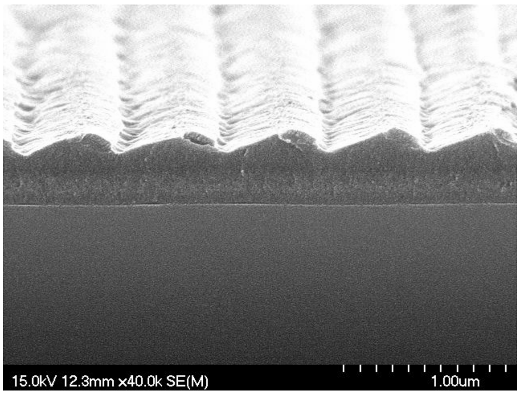 θ =85°
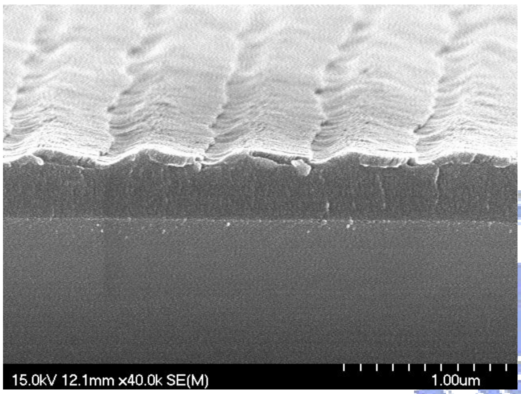 θ =75°	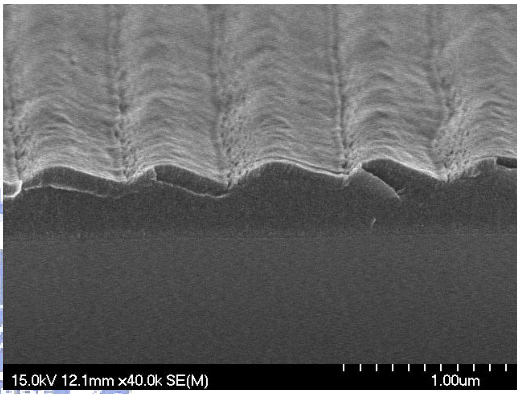 θ =50°

For sample I, the evaporation process is modified by tilting the sample with an angle of 78.69°, while the grating period of the sample is 200 nm and the depth is 40 nm. The evaporation result is shown in Fig. 5.14. The evaporation thickness of Al is 50 nm. The period and the depth of the mold are 198 nm and 70 nm, respectively.

Similarly, for sample II, the evaporation process is modified by tilting the sample with an angle of 78.69°, while the grating period of the sample is 600 nm and the depth is 60nm. The evaporation result is shown in Fig. 5.15. The evaporation thickness of Al is also 50 nm. The period and the depth of the mold are 600 nm and 400 nm, respectively.

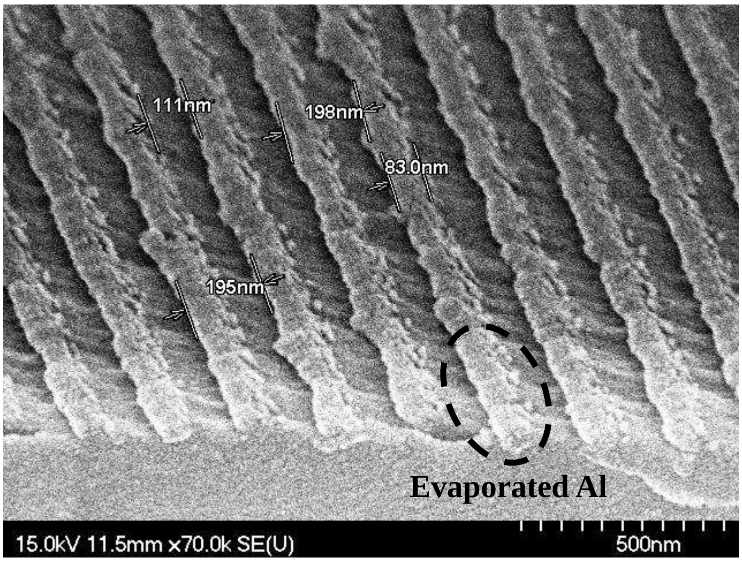

Fig. 5.14 The oblique evaporation result of sample I

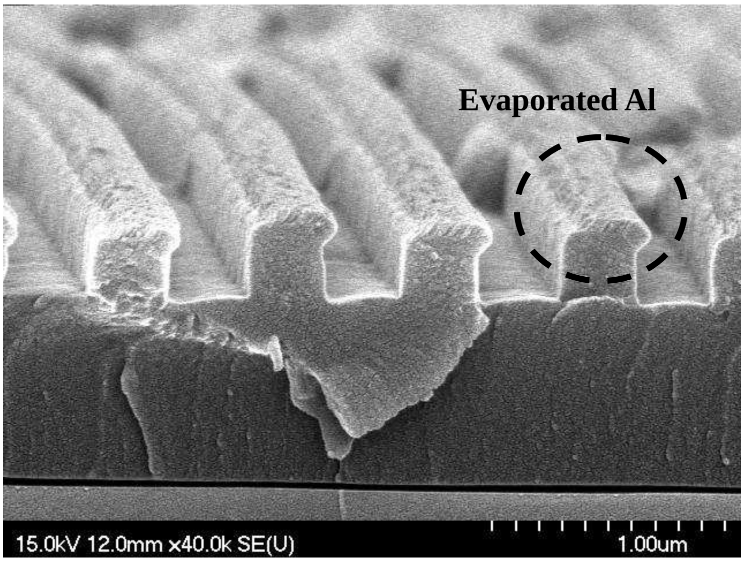

Fig. 5.15 The oblique evaporation result of sample II

5.6 Evaluated Results

We used the measurement setup shown schematically in Fig. 3.13 to evaluate the fabricated sub-wavelength grating with 200 nm period. The measured efficiencies versus wavelength of incident light were shown in Figs. 5.16 and 5.17.

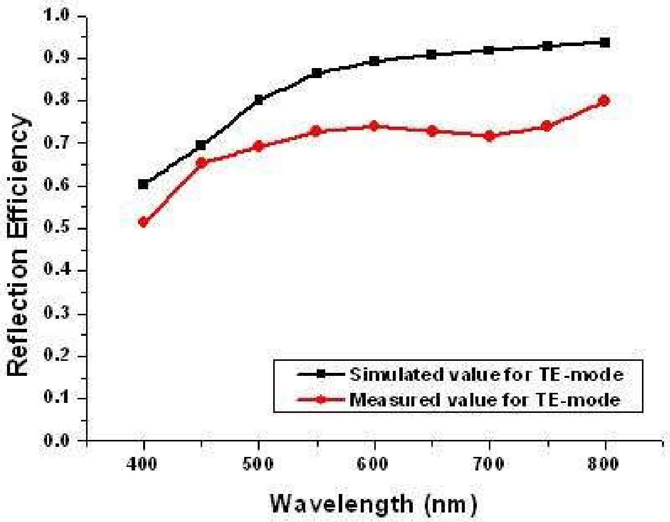

Fig. 5.16 Comparison of measured and calculated results of reflection efficiency versus wavelength of incident light.

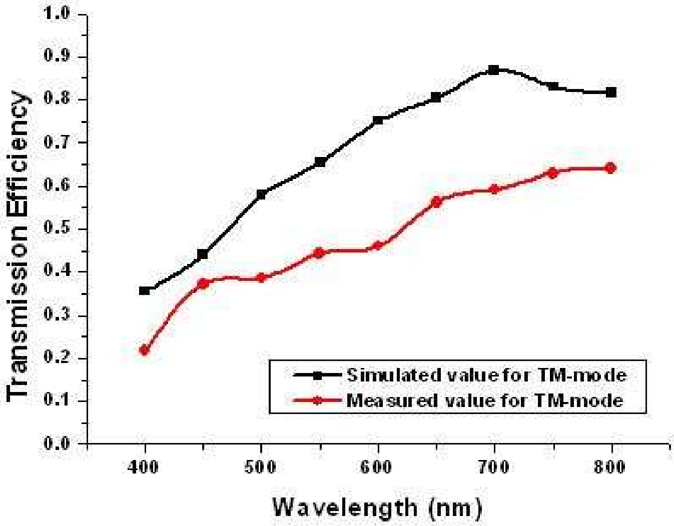

Fig. 5.17 Comparison of measured and calculated results of transmission efficiency versus wavelength of incident light.

Both measured efficiencies, shown in Figs. 5.16 and 5.17, were 30% at most lower than the simulated values, due to slight departures in the actual grating dimensions, shown in Fig. 5.14, from the design. In addition, fabrication defects resulted in a few missing grating features. Besides, the surface roughness might be another issue to affect the efficiency of light separation. Although there were 30% deviations from the simulated values, the measured curves were matched with simulated curves well.

5.7 Discussion

Among the conventional fabrications to produce nanometer-scale pattern, electron beam lithography is one of the best methods by its superior high resolution and focus ability. However, by utilizing e-beam lithography, the fabricated area is usually small, which is about 100μm*100μm. Besides, this lithography is a costly process and relying on a serial fabrication paradigm, making the time needed to produce structures too long for practical industrial use. Owing to the long fabrication time, the throughput can not be mass production.

On the other hand, nanoimprint lithography can improve the defects of E-beam lithography mentioned above. In our fabrication, not only the process time but the fabrication cost can be reduced. In addition, the area of fabricated grating and the yield can be increased more easily. Therefore, if we want to fabricate a large-sized sub-wavelength grating, nanoimprint lithography is a better technique choice.

Tab. 5.3 Comparison between E-beam lithography and nanoimprint lithography

Technique	E-beam direct writing	Nanoimprint lithography
Area of Gating	Small(~100μm*100μm)	Large(1cm*1cm)
Fabrication Time	Several days	~ 3 hours
Fabrication Cost	High	Low
Throughput	Low	High

5.8 Summary

In summary, the creation of vacuum in PDMS conversion process can improve the quality of converted structure and the ability of pattern transferring. During the imprint process, the uniformity of specimen can be improved by controlling the thickness of PDMS mold and pressurizing the slow and smooth gas to the specimen. Besides, the fabrication of angled e-beam evaporation has shown to be a candidate to fabricate a nano-wired grating.